frontiers | Frontiers in Physics

TYPE Perspective
PUBLISHED 16 September 2022
DOI 10.3389/fphy.2022.969806

OPEN ACCESS

EDITED BY
Piergiorgio Cerello,
National Institute of Nuclear Physics of Turin, Italy

REVIEWED BY
Paul Vasos,
University of Bucharest, Romania

*CORRESPONDENCE
Pawel Moskal,
p.moskal@uj.edu.pl
Ewa Ł. Stępień,
e.stepien@uj.edu.pl

SPECIALTY SECTION
This article was submitted to Medical Physics and Imaging, a section of the journal Frontiers in Physics

RECEIVED 15 June 2022
ACCEPTED 29 August 2022
PUBLISHED 16 September 2022

CITATION
Moskal P and Stępień EŁ (2022), Perspectives on translation of positronium imaging into clinics. *Front. Phys.* 10:969806.
doi: 10.3389/fphy.2022.969806

Perspectives on translation of positronium imaging into clinics

Pawel Moskal[1,2,3]* and Ewa Ł. Stępień[1,2,3]*

[1]M. Smoluchowski Institute of Physics, Faculty of Physics, Astronomy and Applied Computer Science, Jagiellonian University, Krakow, Poland, [2]Total-Body Jagiellonian-PET Laboratory, Jagiellonian University, Krakow, Poland, [3]Center for Theranostics, Jagiellonian University, Krakow, Poland

The image of positronium properties created in the patient's body during PET examination tells about the inter- and intra-molecular structure of the tissue and the concentration of bio-active molecules in the tissue [2–4]. In this article, we advocate the opinion that total-body PET systems, thanks to their high imaging sensitivity and high time resolution, open up the prospect of translating positronium imaging into clinics.

KEYWORDS

positronium imaging, biomarkers, medical imaging, J-PET, multi-photon PET, total-body PET, theranostics, hypoxia

Positronium imaging is a newly invented diagnostic method [1–7] with promising potential to improve specificity in the assessment of tissue pathology *in vivo* at the molecular level based on information available from the data collected by the upcoming generation of multi-photon (multi-gamma) PET systems [2, 4, 7, 8].

In general, the development of diagnostic methods in medicine is motivated by the detection of the disease at the early stage, at the level of molecular alterations [9]. Positron emission tomography (PET) is one of the most effective diagnostic methods at the molecular level, before the disease develops into physiological and then structural changes [10]. PET images deliver information on the distribution of the uptake rate of the administered radiopharmaceuticals (e.g., ^{18}F-labeled FDG) and about the expression of specific receptors at cell membranes (e.g., ^{68}Ga-labeled PSMA) [11]. This information comes from the positron–electron annihilation density distribution, which is determined in the patient's body by measuring photons originating from electron–positron annihilation into two photons.

Current PET systems are not sensitive to the annihilation mechanism and dependent on the tissue nanostructure and the concentration of paramagnetic molecules. The availability of information about this mechanism may improve diagnosis. In particular, electron–positron annihilation may proceed not only directly but also through the formation of a metastable positronium atom. A positronium is an atom composed of a positron and an electron, which is formed in about 40% of cases of annihilation in inter- and intra-molecular voids during PET examination [3]. The mean lifetime and the probability of positronium production depend on the size of inter- and intra-molecular spaces and the concentration of paramagnetic molecules, such as O_2, therein. Therefore, imaging of positronium properties such as mean lifetime or production probability provides information that is independent and complementary to the standardized uptake value (SUV) currently available in PET imaging.

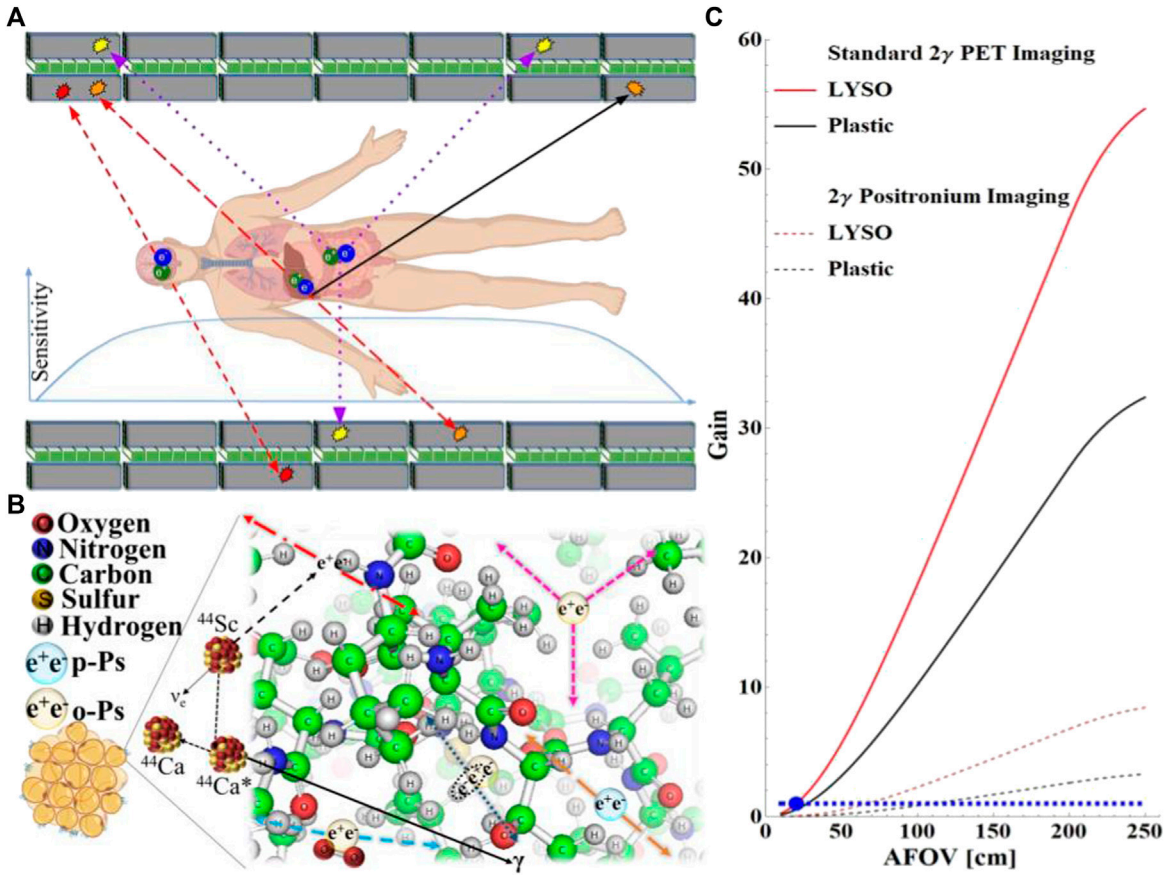

FIGURE 1
(A) Axial cross section of the design scheme of the multi-photon total-body J-PET scanner consisting of seven rings with axially arranged scintillators. Each ring consists of 24 modules composed of two layers of scintillators (gray rectangles) and the layer of WLS fibers (green squares). Superimposed chart indicates the sensitivity profile [4]. The superimposed arrows indicate three exemplary annihilation events. Two-photon annihilation (red dashed arrows), two-photon annihilation (red long dashed arrows) accompanied with the deexcitation photon (black solid arrow), and three-photon annihilation (blue dotted arrows) are shown. **(B)** Pictorial representation of various mechanisms responsible for the positronium annihilation in the adipose tissue. Positron (dashed arrow) is emitted by the 44Sc radionuclide which after transformation to ^{44}Ca emits a deexcitation photon (black arrow). Direct annihilation is indicated with red long-dashed dotted arrows. Violet arrows indicate self-annihilation of ortho-positronium into three photons. Dashed brown arrows show self-annihilation of para-positronium into two photons. Blue dotted arrows indicate pick-off annihilation of the positron from positronium with the electron from the molecule, and the dashed blue arrows indicate two-photon annihilation of para-positronium produced as a result of the conversion of ortho-positronium into para-positronium on the oxygen molecule. **(C)** Sensitivity gain with respect to the 20-cm-long PET built from LYSO crystals (blue dot). Red and black curves represent the results for LYSO and plastic scintillators, respectively. The horizontal dashed line indicates gain equal to unity for guiding the eye. The meaning of the curves is explained in the legend. Solid red and black curves represent the sensitivity gain for standard two-photon imaging as a function of the axial field-of-view (AFOV) for the LYSO-based PET (1.81 cm thick) and for the plastic (J-PET as shown in panel A with 3-cm-thick plastic strips), respectively. Dotted curves indicate the result for the positronium imaging based on the registration of two annihilation photons and the prompt gamma.

Positronium imaging with multi-photon positron emission tomography scanners

Over six decades of continuous development, PET technology has led to the development of total-body PET systems capable of simultaneously imaging all tissues and organs in the human body [12, 13]. The high sensitivity of total-body PET in the registration of two-photon annihilation enables dynamic model- and kinetic model-based parametric imaging, which increases the specificity of the diagnosis of the disease, especially with regard to the differentiation between neoplastic and inflammatory tissues [10]. The exceptionally high sensitivity of total-body PET systems also enables the effective registration of positronium annihilation into three photons and the simultaneous registration of two photons from the electron–positron annihilation and deexcitation photons [4], which is graphically illustrated in Figure 1. Panel A, on the example of the design of the total-body J-PET system, presents the processes relevant for standard two-photon PET imaging as well as three-photon processes essential for positronium imaging. Panel B indicates the basic

processes leading to the annihilation of positronium in the tissue, where electron–positron annihilation proceeds through positronium formation in approximately 30–40% of cases [3.4]. A quarter of positronia are produced as short-lived para-positronium with a mean lifetime in vacuum of 125 ps, and three-quarters of positronia are produced as long-lived ortho-positronium with the mean lifetime in vacuum of 142 ns [5, 6]. In tissues, the positronium lifetime of ortho-positronium is significantly shortened due to the pick-off and conversion processes indicated in panel B in Figure 1. The smaller the inter- and intra-molecular voids, the shorter the mean ortho-positronium lifetime and the lower the fraction of the decay rate of three to two photons. Moreover, the higher the oxygen concentration, the shorter the mean ortho-positronium lifetime and the lower the three-photon to two-photon decay rate ratio. Therefore, the mean lifetime of ortho-positronium and the ratio of the three-photon to two-photon decay rates may be used as a biomarker of tissue alteration at the molecular level and as a biomarker of hypoxia [14]. The ratio of the rate of decay of three photons to two photons can be determined for all kinds of positron-emitting radionuclides. However, to determine the mean lifetime of ortho-positronium, a special class of isotopes is needed, which apart from the positron also emit the so-called prompt gamma, such as scandium-44 [4, 15, 16]. The isotope ^{44}Sc is the most suitable radionuclide for this purpose because almost 100% of positron (e^+) emission is accompanied by prompt gamma (γ) emission through the decay chain: $^{44}\mathrm{Sc} \rightarrow {}^{44}\mathrm{Ca}^{*}\ e^+\ \nu \rightarrow {}^{44}\mathrm{Ca}\ \gamma\ e^+\ \nu$ [16] (Figure 1B), where ^{44}Ca* denotes the excited calcium-44 isotope and v denotes the neutrino. The prompt gamma is emitted on average in about 3 ps after positron emission, and the thermalization of the positron in tissue also takes only a few ps. Therefore, the lifetime of a positronium may be well approximated by the time difference between the time of annihilation and the time of prompt gamma emission. These times can be determined by measuring annihilation photons and prompt gamma. The method has been described in detail in Refs. [2, 5, 6, 17].

^{44}Sc can be obtained from the ^{44}Ti/^{44}Sc generator and by the ^{44}Ca $(p,n)^{44}$Sc nuclear reaction [18]. ^{44}Sc has beneficial properties in the diagnosis of cancer with PET. Scandium-44 could be used as an alternative to the currently used ^{68}Ga (T1/2 = 68.3 min), with a longer half-life ($T_{1/2}$ = 4.04 h), which would improve image quality [19, 20], when images are recorded at later time points (when tumor-to-background ratios are enhanced) [21]. ^{44}Sc has been extensively used in preclinical studies using various targeting agents, such as folates [19, 20], somatostatin analogs [22], and PSMA-targeted ligands [23].

The first positronium images have recently been demonstrated using the J-PET multi-photon scanner prototype [2, 7]. J-PET tomograph was enabled to reconstruct positronium images for both three-photon annihilations [7] and two-photon pick-off annihilations of ortho-positronium [2], showing that both positronium lifetime imaging and imaging of the three-photon to two-photon rate ratios are feasible. Figure 1C compares the sensitivity of two-photon positronium imaging with standard two-photon PET imaging. The figure shows the gain in sensitivity as a function of the scanners' axial field-of-view. The sensitivity of positronium lifetime imaging is approximately 10 times lower than that of standard two-photon PET examinations. This is because in positronium lifetime imaging, in addition to the two annihilation photons, a prompt gamma must be registered. Moreover, it can be seen (as it was recently discussed in the literature [4, 14]) that in the case of the total-body PET systems, the sensitivity of positronium imaging is even higher than the sensitivity of the 20-cm-long standard two-photon PET systems.

Positronium as a biomarker of cancer and hypoxia

The properties of the positronium, such as the mean lifetime and the three-photon to two-photon decay ratio, are sensitive to the nanostructure of the tissue and oxygen concentration in the tissue [3]. It is worth noting that there are studies demonstrating that these properties are also correlated with changes at the level of cellular physiology [2, 24–32]. In tissues, the mean lifetime of ortho-positronium varies from about 1.8 ns in water to about 4 ns in human skin. The observed differences in the mean lifetime expectancy of ortho-positronium between healthy and cancer tissues, ranging from 50 to 700 ps, are the most promising for positronium applications as a biomarker [2, 25, 33–35]. For example, the mean lifetime of ortho-positronium in cardiac myxoma tumor tissues is shorter by about 700 ps than the mean ortho-positronium lifetime in healthy adipose tissues [2, 25]. It has also been demonstrated that positronium lifetime changes inversely to the oxygen concentration in organic liquids [36, 37] and can be considered a biomarker of hypoxia [14]. The partial pressure of oxygen in neoplastic tissues is lower by more than 10 mmHg with respect to healthy tissues of the same organ, and for the pancreas, the difference is as high as 50 mmHg [38]. In order to distinguish such an oxygen pressure difference, an ortho-positronium lifetime resolution of about 2 ps is required [14]. The time resolution of reconstruction of the mean ortho-positronium lifetime in a given image voxel depends predominantly on the statistics of events in this voxel (N) and the value of the mean lifetime (τ_{oPs}), and therefore it can be estimated as τ_{oPs}/sqrt(N) [6]. For total-body PET imaging, approximately 10^4 events are expected in the cm^3 voxel of the positronium image [6]. This results in a resolution of τ_{oPs} reconstruction of approximately 20 ps. Such precision, already achieved in the first *in vitro* positronium images of cardiac myxoma and adipose tissues [2], is sufficient to disentangle the differences between healthy and neoplastic tissues in the region of interest (ROI) of several cubic centimeters. Moreover, it is also sufficient to distinguish between hypoxic and normoxic conditions organ-wise by integrating events from volumes of 100 cm^3 or larger, for example, for the pancreas or liver [14]. It is important to stress that the recently developed PALS Avalanche software program enables fast online analysis and decomposition of positronium annihilation lifetime spectra [39], and moreover it has been demonstrated that

iterative numerical inverse Laplace transform algorithms with Tikhonov regularization enable to distinguish lifetime components in the positronium images differing by only ~5 ps [40].

The spatial resolution of the direct positronium image reconstruction depends predominantly on the time resolution of the PET system. The very first positronium image recently demonstrated using a multi-photon J-PET tomograph was reconstructed with the coincidence resolving time resolution (CRT) of about 500 ps, corresponding to a spatial resolution of 75 mm [2, 7]. It is worth noting that the time resolution of PET systems is constantly improving, and there is also the ongoing rapid development of new materials with improved timing properties [41, 42] and new detectors for preclinical [43] and clinical [2, 8, 44–46] studies. The best current clinical time-of-flight (TOF)-PET systems [47] are characterized by CRT of 210 ps, equivalent to a position resolution of about 32 mm along the line of response. On the other hand, laboratory detectors already achieved a CRT of even 30 ps (corresponding to a position resolution of 4.5 mm) [48], and the first direct PET images of the two-dimensional Hoffman brain phantom were experimentally demonstrated with the spatial precision of 4.8 mm [49]. Moreover, recently, on the basis of simulated 2D data, it has been shown that the statistical approach using the panelized maximum likelihood image estimation method enables to achieve a spatial resolution of the positronium image better than 4 mm, even for PET systems with CRT of 570 ps [50, 51]. Thus, high-quality positronium images are at present achievable with the total-body PET scanners such as EXPLORER (CRT ~500 ps) [44], PennPET EXPLORER (CRT ~260 ps) [45], or Vision Quadra (CRT ~230 ps) [52, 53], provided that the acquisition systems are modified to detect triple coincidences with an extension of energy window for prompt gamma registration.

Conclusion

In this opinion article, we discussed the current state of development of newly invented positronium imaging requiring high sensitivity and high-time-resolution multi-photon PET systems [1–7]. By reviewing the latest advances in the development of total-body and multi-photon PET systems, we have shown that the current PET technology is ready for effective positronium imaging in clinics with the spatial resolution comparable to that of the current PET images. In fact, the first clinical positronium images have recently been demonstrated [46]. The achieved time and spatial resolution make a promising prospect that positronium may serve as an *in vivo* biomarker to assess tissue pathology and the degree of hypoxia [2, 13, 25, 36, 54]. *In vivo* hypoxia studies are crucial for effective cancer treatment [55].

The properties of positronium are sensitive to the inter- and intra-molecular structure and the concentration of bio-active molecules in the inter- and intra-molecular voids; therefore, they may turn out to be sensitive to functional cell alteration at the molecular level reflected in nanostructural changes. Density distribution of radiopharmaceutical, currently available from PET examination, reflects the rate of cellular metabolism or the expression of receptors with an affinity to the administered radioligand. The positronium biomarker may provide additional diagnostic information for differentiation of neoplastic and inflammatory lesions, since changes at the molecular level accompanying neoplastic disease do not necessarily occur in the case of inflammatory diseases [44–46, 51–56]. The observed high mean lifetime for adipose tissues [2, 19–32] may make positronium an effective biomarker for noninvasive assessment of liver diseases, for e.g., liver fibrosis, fatty liver disease, or non-alcoholic fatty liver diseases [44–46, 52–57], and for the early diagnosis of pancreatic cancer or renal fibrosis [45, 46, 52–58]. In general, positronium imaging may open up a new paradigm of hitherto unexplored early diagnosis and assessment of the tissue pathology in all organs *in vivo*.

Data availability statement

The original contributions presented in the study are included in the article/Supplementary Material; further inquiries can be directed to the corresponding authors.

Author contributions

All authors listed have made a substantial, direct, and intellectual contribution to the work and approved it for publication.

Funding

The authors acknowledge support from the Foundation for Polish Science under the TEAM POIR.04.04.00-00-4204/17 program, the National Science Centre of Poland under grant nos. 2019/33/B/NZ3/01004, 2021/42/A/ST2/00423, and 2021/43/B/ST2/02150 as well as the SciMat and qLife Priority Research Areas budget under the program Excellence Initiative—Research University at the Jagiellonian University, and Jagiellonian University under project no. CRP/0641.221.2020.

Acknowledgments

The authors thank D. Panek, Sz. Parzych, and Shivani for helping with the preparation of figures.

Conflict of interest

The authors declare that the research was conducted in the absence of any commercial or financial relationships that could be construed as a potential conflict of interest.

Publisher's note

References

1. Moskal P. Positronium imaging. In: 2019 IEEE Nuclear Science Symposium and Medical Imaging Conference (NSS/MIC). Manchester, UK: IEEE Xplore (2020). doi:10.1109/NSS/MIC42101.2019.9059856

2. Moskal P, Dulski K, Chug N, Curceanu C, Czerwiński E, Dadgar M, et al. Positronium imaging with the novel multiphoton PET scanner. *Sci Adv* (2021) 7: eabh4394. doi:10.1126/sciadv.abh4394

3. Moskal P, Jasińska B, Stępień EŁ, Bass S. Positronium in medicine and biology. *Nat Rev Phys* (2019) 1:527–9. doi:10.1038/s42254-019-0078-7

4. Moskal P, Stępień EŁ. Prospects and clinical perspectives of total-body PET imaging using plastic scintillators. *PET Clin* (2020) 15:439–52. doi:10.1016/j.cpet.2020.06.009

5. Moskal P, Kisielewska D, Curceanu C, Czerwiński E, Dulski K, Gajos A, et al. Feasibility study of the positronium imaging with the J-PET tomograph. *Phys Med Biol* (2019) 64:055017. doi:10.1088/1361-6560/aafe20

6. Moskal P, Kisielewska D, Bura Z, Chhokar J, Curceanu C, Czerwiński E, et al. Performance assessment of the 2 γpositronium imaging with the total-body PET scanners. *EJNMMI Phys* (2020) 7:44. doi:10.1186/s40658-020-00307-w

7. Moskal P, Gajos A, Mohammed M, Chhokar J, Chug N, Curceanu C, et al. Testing CPT symmetry in ortho-positronium decays with positronium annihilation tomography. *Nat Commun* (2021) 12:5658. doi:10.1038/s41467-021-25905-9

8. Niedźwiecki S, Białas P, Curceanu C, Czerwiński E, Dulski K, Gajos A, et al. J-PET: A new technology for the whole-body PET imaging. *Acta Phys Pol B* (2017) 48:1567. doi:10.5506/aphyspolb.48.1567

9. Rivenbark AG, O'Connor SM, Coleman WB. Molecular and cellular heterogeneity in breast cancer: Challenges for personalized medicine. *Am J Pathol* (2013) 183:1113–24. doi:10.1016/j.ajpath.2013.08.002

10. Alavi A, Werner TJ, Stępień EŁ, Moskal P. Unparalleled and revolutionary impact of PET imaging on research and day to day practice of medicine. *Bio-Algorithms and Med-Systems* (2021) 17:203–12. doi:10.1515/bams-2021-0186

11. Królicki L, Kunikowska J. Theranostics – present and future. *Bio-Algorithms and Med-Systems* (2021) 17:213–20. doi:10.1515/bams-2021-0169

12. Vandenberghe S, Moskal P, Karp JS. State of the art in total body PET. *EJNMMI Phys* (2020) 7:35. doi:10.1186/s40658-020-00290-2

13. Badawi RD, Shi H, Hu P, Chen S, Xu T, Price PM, et al. First human imaging studies with the EXPLORER total-body PET scanner. *J Nucl Med* (2019) 60: 299–303. doi:10.2967/jnumed.119.226498

14. Moskal P, Stępień EŁ. Positronium as a biomarker of hypoxia. *Bio-Algorithms and Med-Systems* (2021) 17:311–9. doi:10.1515/bams-2021-0189

15. Matulewicz T. Radioactive nuclei for β+γ PET and theranostics: Selected candidates. *Bio-Algorithms and Med-Systems* (2021) 17:235–9. doi:10.1515/bams-2021-0142

16. Choiński J, Łyczko M. Prospects for the production of radioisotopes and radiobioconjugates for theranostics. *Bio-Algorithms and Med-Systems* (2021) 17: 241–57. doi:10.1515/bams-2021-0136

17. Moskal P, Moskal I, Moskal G. *TOF-PET tomograph and a method of imaging using a TOF-PET tomograph, based on a probability of production and lifetime of a positronium*. Patent No. PL 227658 (2018), EP 3039453 (2020), US 9, 851, 456 (2017) (2017).

18. Pruszyński M, Loktionova NS, Filosofov DV, Roesch F. Post-elution processing of 44Ti/44Sc generator-derived 44Sc for clinical application. *Appl Radiat Isot* (2010) 68:1636–41. doi:10.1016/j.apradiso.2010.04.003

19. Müller C, Bunka M, Reber J, Fischer C, Zhernosekov K, Türler A, et al. Promises of cyclotron-produced 44Sc as a diagnostic match for trivalent β−-emitters: *In vitro* and *in vivo* study of a 44Sc-DOTA-Folate conjugate. *J Nucl Med* (2013) 54:2168–74. doi:10.2967/jnumed.113.123810

20. Van der Meulen NP, Bunka M, Domnanich KA, Müller C, Haller S, Vermeulen C, et al. Cyclotron production of 44Sc: From bench to bedside. *Nucl Med Biol* (2015) 42:745–51. doi:10.1016/j.nucmedbio.2015.05.005

21. Singh A A, Van der Meulen NP, Müller C, Klette I, Kulkarni HR, Türler A, et al. First-in-Human PET/CT imaging of metastatic neuroendocrine neoplasms with cyclotron-produced ^{44}Sc-dotatoc: A proof-of-concept study. *Cancer Biother Radiopharm* (2017) 32:124–32. doi:10.1089/cbr.2016.2173

22. Müller C, Domnanich AK, Umbricht CA, Van der Meulen NP. Scandium and terbium radionuclides for radiotheranostics: Current state of development towards clinical application. *Br J Radiol* (2018) 91:20180074. doi:10.1259/bjr.20180074

23. Umbricht C, Benešová M, Schmid RM, Türler A, Schibli R, Van der Meulen NP, et al. 44Sc-PSMA-617 for radiotheragnostics in tandem with 177Lu-PSMA-617—Preclinical investigations in comparison with 68Ga-PSMA-11 and 68Ga-PSMA-617. *EJNMMI Res* (2017) 7:9–10. doi:10.1186/s13550-017-0257-4

24. Stępień EŁ, Kubicz E, Grudzień G, Dulski K, Leszczyński B, Moskal P. Positronium life-time as a new approach for cardiac masses imaging. *Eur Heart J* (2021) 42:ehab724.3279. doi:10.1093/eurheartj/ehab724.3279

25. Moskal P, Kubicz E, Grudzień G, Czerwiński E, Dulski K, Leszczyński B, et al. Developing a novel positronium biomarker for cardiac myxoma imaging. *bioRxiv* (2021) 2021:455285. doi:10.1101/2021.08.05.455285

26. Zgardzińska B, Chołubek G, Jarosz B, Wysogląd K, Gorgol M, Goździuk M, et al. Studies on healthy and neoplastic tissues using positron annihilation lifetime spectroscopy and focused histopathological imaging. *Sci Rep* (2020) 10:11890. doi:10.1038/s41598-020-68727-3

27. Chen HM, van Horn JD, Jean YC. Applications of positron annihilation spectroscopy to life science. *Defect Diffusion Forum* (2012) 331:275–93. doi:10.4028/www.scientific.net/ddf.331.275

28. Jasińska B, Zgardzińska B, Chołubek G, Pietrow M, Gorgol M, Wiktor K, et al. Human tissue investigations using PALS technique - free radicals influence. *Acta Phys Pol A* (2017) 132:1556–9. doi:10.12693/aphyspola.132.1556

29. Kilburn D, Townrow S, Meunier V, Richardson R, Alam A, Ubbink J. Organization and mobility of water in amorphous and crystalline trehalose. *Nat Mater* (2006) 5:632–5. doi:10.1038/nmat1681

30. Jean YC, Li Y, Liu G, Chen H, Zhang J, Gadzia JE. Applications of slow positrons to cancer research: Search for selectivity of positron annihilation to skin cancer. *Appl Surf Sci* (2006) 252:3166–71. doi:10.1016/j.apsusc.2005.08.101

31. Axpe E, Lopez-Euba T, Castellanos-Rubio A, Merida D, Garcia JA, Plaza-Izurieta L, et al. Detection of atomic scale changes in the free volume void size of three-dimensional colorectal cancer cell culture using positron annihilation lifetime spectroscopy. *PLoS One* (2014) 9:e83838. doi:10.1371/journal.pone.0083838

32. Avachat AV, Leja AG, Mahmoud KH, Anastasio MA, Sivaguru M, Di Fulvio A. *Positron annihilation lifetime spectroscopy of adipose, hepatic, and muscle tissues* (2022). doi:10.21203/rs.3.rs-1657111/v1

33. Liu G, Chen H, Chakka L, Gadzia JE, Jean YC. Applications of positron annihilation to dermatology and skin cancer. *Phys Status Solidi* (2007) 4:3912–5. doi:10.1002/pssc.200675736

34. Pietrzak R, Borbulak S, Szatanik R. Influence of neoplastic therapy on the investigated blood using positron annihilation lifetime spectroscopy. *Nukleonika* (2013) 58:199–202.

35. Jasińska B, Zgardzińska B, Chołubek G, Gorgol M, Wiktor K, Wysogląd K, et al. Human tissues investigation using PALS technique. *Acta Phys Pol B* (2017) 48: 1737. doi:10.5506/aphyspolb.48.1737

36. Shibuya K, Saito H, Nishikido F, Takahashi M, Yamaya T. Oxygen sensing ability of positronium atom for tumor hypoxia imaging. *Commun Phys* (2020) 3: 173–8. doi:10.1038/s42005-020-00440-z

37. Stepanov P, Selim F, Stepanov S, Bokov A, Ilyukhina O, Duplâtre G, et al. Interaction of positronium with dissolved oxygen in liquids. *Phys Chem Chem Phys* (2020) 22:5123–31. doi:10.1039/c9cp06105c

38. Vaupel P, Flood AB, Swartz HM. Oxygenation status of malignant tumors vs. Normal tissues: Critical evaluation and updated data source based on direct measurements with pO2 microsensors. *Appl Magn Reson* (2021) 52:1451–79. doi:10.1007/s00723-021-01383-6

39. Dulski KOn Behalf of the J-PET Collaboration. PALS Avalanche - a new PAL spectra analysis software. *Acta Phys Pol A* (2020) 137:167–70. doi:10.12693/aphyspola.137.167

40. Shibuya K, Saito H, Tashima H, Yamaya T. Using inverse Laplace transform in positronium lifetime imaging. *Phys Med Biol* (2022) 67:025009. doi:10.1088/1361-6560/ac499b

41. Lecoq P, Konstantinou G, Latella R, Moliner L, Nuyts J, Zhang L, et al. Metascintillators: New results for TOF-PET applications. *IEEE Trans Radiat Plasma Med Sci* (2022) 6:510. doi:10.1109/trpms.2022.3161473

42. Lecoq P, Morel C, Prior J, Visvikis D, Gundacker S, Auffray E, et al. Roadmap toward the 10 ps time-of-flight PET challenge. *Phys Med Biol* (2020) 65:21RM01. doi:10.1088/1361-6560/ab9500

43. Jegal J, Jeong D, Seo ES, Park HW, Kim H. Convolutional neural network-based reconstruction for positronium annihilation localization. *Sci Rep* (2022) 12: 8531. doi:10.1038/s41598-022-11972-5

44. Spencer BA, Berg E, Schmall JP, Omidvari N, Leung EK, Abdelhafez YG, et al. Performance evaluation of the uEXPLORER total-body PET/CT scanner based on NEMA NU 2-2018 with additional tests to characterize PET scanners with a long axial field of view. *J Nucl Med* (2021) 62:861–70. doi:10.2967/jnumed.120.250597

45. Karp JS, Viswanath V, Geagan MJ, Muehllehner G, Pantel AR, Parma MJ, et al. PennPET explorer: Design and preliminary performance of a whole-body imager. *J Nucl Med* (2020) 61:136–43. doi:10.2967/jnumed.119.229997

46. Moskal P. First clinical positronium imaging of patients. In: Presentation at the 4th Jagiellonian Symposium on Advances in Particle Physics and Medicine; 10-15 July, 2022; Cracow, Poland (2022).

47. van Sluis J, de Jong J, Schaar J, Noordzij W, van Snick P, Dierckx R, et al. Performance characteristics of the digital biograph vision PET/CT system. *J Nucl Med* (2019) 60:1031–6. doi:10.2967/jnumed.118.215418

48. Ota R, Nakajima K, Ogawa I, Tamagawa Y, Shimoi H, Suyama M, et al. Coincidence time resolution of 30 ps FWHM using a pair of Cherenkov-radiator integrated MCPPMTs. *Phys Med Biol* (2019) 64:07LT01. doi:10.1088/1361-6560/ab0fce

49. Kwon SI, Ota R, Berg E, Hashimoto F, Nakajima K, Ogawa I, et al. Ultrafast timing enables reconstruction-free positron emission imaging. *Nat Photon* (2021) 15:914–8. doi:10.1038/s41566-021-00871-2

50. Qi J, Huang B. Positronium lifetime image reconstruction for TOF PET. *IEEE Trans Med Imaging* (2022). doi:10.1109/TMI.2022.3174561

51. Zhu Z, Harrison CW, Kao C-M, Huang H-H. *A statistical reconstruction algorithm for positronium lifetime imaging using time-of-flight positron emission tomography* (2022). arXiv:2206.06463v1 [physics.med-ph] 13 Jun 2022.

52. Alberts I, Hünermund JN, Prenosil G, Mingels C, Bohn KP, Viscione M, et al. Clinical performance of long axial field of view PET/CT: A head-to-head intra-individual comparison of the biograph vision Quadra with the biograph vision PET/CT. *Eur J Nucl Med Mol Imaging* (2021) 48:2395–404. doi:10.1007/s00259-021-05282-7

53. Prenosil GA, Sari H, Fürstner M, Afshar-Oromieh A, Shi K, Rominger A, et al. Performance characteristics of the biograph vision Quadra PET/CT system with a long axial field of view using the NEMA NU 2-2018 standard. *J Nucl Med* (2022) 63: 476–84. doi:10.2967/jnumed.121.261972

54. Zare M, Ghasemi B, Kakuee O, Biganeh A. Experimental investigation of the oxygen sensing ability of positron annihilation spectroscopy for tumor imaging. *Radiat Phys Eng* (2022) 3:1–5. doi:10.22034/rpe.2022.336848.1072

55. Cramer T, Vaupel P. Severe hypoxia is a typical characteristic of human hepatocellular carcinoma: Scientific fact or fallacy? *J Hepatol* (2022) 76:975–80. doi:10.1016/j.jhep.2021.12.028

56. Rahman WT, Wale DJ, Viglianti BL, Townsend DM, Manganaro MS, Gross MD, et al. The impact of infection and inflammation in oncologic 18F-FDG PET/CT imaging. *Biomed Pharmacother* (2019) 117:109168. doi:10.1016/j.biopha.2019.109168

57. Cleveland E, Bandy A, VanWagner LB. Diagnostic challenges of nonalcoholic fatty liver disease/nonalcoholic steatohepatitis. *Clin Liver Dis (Hoboken)* (2018) 11: 98–104. doi:10.1002/cld.716

58. Zhang J, Yu Y, Liu X, Tang X, Xu F, Zhang M, et al. Evaluation of renal fibrosis by mapping histology and magnetic resonance imaging. *Kidney Dis (Basel)* (2021) 7: 131–42. doi:10.1159/000513332